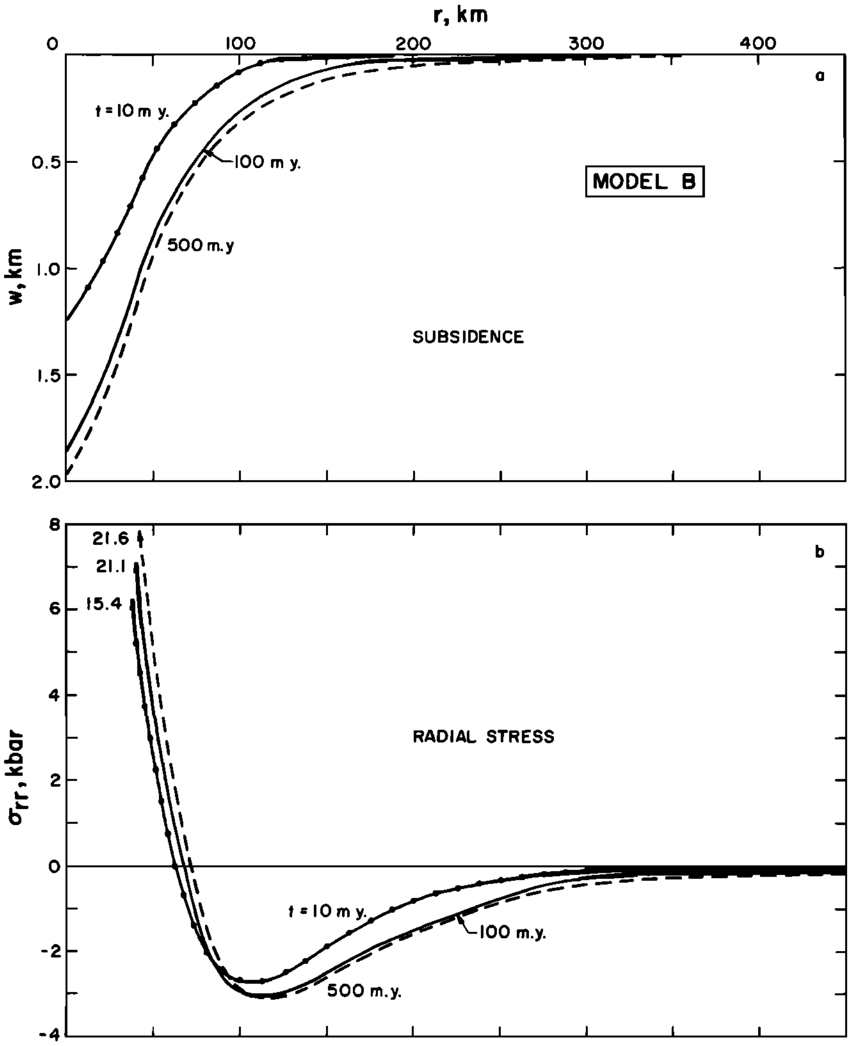

Fig. 14. Surface subsidence w and radial thermal stress σ_{rr} for basin thermal model B (Figure 12). Curves shown represent accumulated values at 10, 100, and 500 m.y. after basin formation.

models B and C in Figures 14 and 15, respectively. Shown in each figure are w and σ_{rr} at the lunar surface versus r and t. The shapes of the curves for u and $\sigma_{\theta\theta}$ and their relationships to w and σ_{rr} are similar to those for model A (Figure 11).

Comparison of Figures 14 and 15 shows that the patterns of accumulated displacement and stress reflect the distribution of initial heat (defined by s) in each model. Most of the subsidence in model B is confined to the first 100 m.y. and to radial distances less than 150 km. Subsidence near $r = 0$ (Figure 14*a*) is 1.8 km by 100 m.y. Subsidence beneath the basin center for model C (Figure 14*a*) is lower in magnitude (only ~0.2 km by 100 m.y.) but takes place over a broader region. Also, because heat is lost more slowly in model C, a significant proportion of the total subsidence takes place between 100 and 500 m.y. Accumulated radial stress (Figures 14*b* and 15*b*) in the center of both models is compressional and exceeds 1 kbar. Maximum extensional stress in model B occurs between $r = 90$ and 130 km and accumulates to about -3 kbar. The distribution of σ_{rr} in model C contains a relatively broader region of extension; maximum accumulated extensional stress is -0.2 kbar at 100 m.y.

Neither model B nor model C satisfactorily predicts the location of fissures within Orientale or matches the full magnitude of relief of the central depression. However, these models indicate the sensitivity of the displacement and stress fields to the values of the parameters E_B and s. The magnitudes of displacement and thermal stress scale linearly with E_B, but the distributions of those quantities depend on s. Therefore, if some portion of the relief of the central depression and the band of fissures are products of thermal stress and if the elastic half-space model adequately represents the response of the moon during the time of basin formation and modification, we may constrain the quantity and distribution of heat implanted during basin formation by varying s so as to match the horizontal extent of the central depression and the locus of fissuring and varying E_B so as to match a given fraction of the relief of the central depression. Of course, it is important to keep in mind that the effects of isotherm uplift (e.g., model A) will have to be added to the effects of impact heating to estimate the total thermoelastic response of the moon to the basin formation event.

A model for impact heating following the above guidelines, model D, is shown in Figure 16*a*. For this model $E_B = 7 \times 10^{32}$ erg and $s = 50$ km. Significant impact heating extends to radial distances and depths comparable to the radius of Orientale (310 km). Near-surface temperatures within 150 km of basin center exceed the liquidus temperatures of most igneous rocks; the rate of cooling in this model is underesti-